JACS
JOURNAL OF THE AMERICAN CHEMICAL SOCIETY
Communication
pubs.acs.org/JACS

Subporphyrinato Boron(III) Hydrides

Eiji Tsurumaki,[†] Jooyoung Sung,[‡] Dongho Kim,*[,‡] and Atsuhiro Osuka*[,†]

[†]Department of Chemistry, Graduate School of Science, Kyoto University, Sakyo-ku, Kyoto 606-8502, Japan

[‡]Spectroscopy Laboratory for Functional π-Electronic Systems and Department of Chemistry, Yonsei University, Seoul 120-749, Korea

Supporting Information

ABSTRACT: Subporphyrinato boron(III) hydrides were prepared by reduction of subporphyrinato boron(III) methoxides with diisobutylaluminum hydride (DIBAL-H) in good yields. The authenticity of the B−H bond has been unambiguously confirmed by a ^{1}H NMR signal that appears as a broad quartet at −2.27 ppm with a large coupling constant with the central ^{11}B, characteristic B−H infrared stretching frequencies, and single crystal X-ray diffraction analysis. Red shifts in the corresponding absorption and fluorescence profiles are accounted for in terms of the electron-donating nature of the B-hydride. The hydridic character of subporphyrinato boron(III) hydrides has been demonstrated by the production of H_2 via reaction with water or HCl, and controlled reductions of aromatic aldehydes and imines in the presence of a catalytic amount of $Ph_3C[B(C_6F_5)_4]$.

In recent years, subporphyrin, a ring-contracted 14π-porphyrin cousin consisting of three pyrrole units connected via three methine carbon atoms, has emerged as a new class of functional pigments.[1−4] While subporphyrins and porphyrins share many common attributes such as strong absorption, fluorescence, and aromaticity, the former bears an axial B-substituent that can be used for fine-tuning the overall reactivities and electronic properties. Different from subphthalocyanines, a ring-contracted 14π-phthalocyanine cousin,[1c,5] the axial substituent of subporphyrin can be readily exchanged as depicted in Scheme 1. Subporphyrinato boron(III) methoxide (hereinafter referred to as subporphyrin B-methoxide) **1** can be quantitatively converted into subporphyrin B-hydroxide **2** upon treatment with an aqueous HCl solution, while heating **2** in the presence of an excess amount of methanol regenerates **1**.[2a,b,4] Subporphyrin **2** can be converted to subporphyrin B-fluoride **3** upon treatment with an excess amount of $BF_3{\cdot}OEt_2$.[4c] Furthermore, B-arylated subporphyrin **5** can be prepared from the reaction of **1** with the appropriate Grignard reagent,[4e] and subporphyrin borenium cation **4** can be isolated as a stable salt with a noncoordinating carborane counteranion.[4d]

Subporphyrin B-hydride is a new and promising variant that may be utilized as a reducing reagent or may possess interesting properties. However, due to the difficulty of preparation, examples of B-hydrides of porphyrinoids have remained elusive in the literature thus far. While a considerable body of work by Brothers et al. documents the synthesis and reactivity of boron porphyrins,[6a,b] a diboron-coordinated corrole was reported as the sole example of such a species.[6c] In this paper, we disclose the first synthesis of subporphyrin B-hydrides.

Initial attempts to synthesize subporphyrin B-hydride **6** involved reactions of **1** with various hydride reducing agents. While **1** was unreactive toward $NaBH_4$, even in refluxing THF, treatment of **1** with $LiAlH_4$ at 0 °C resulted in over-reduction to give a complex mixture, from which it was possible to isolate a trace amount of **6**. The yield of hydride transfer was increased to 20% when using $LiAlH_4$ in a 1:1 mixture of THF/CH_2Cl_2. Finally, we found that DIBAL-H was the optimum hydride delivery reagent, as **6** was produced in 94% yield when the reduction was performed with 20 equiv of DIBAL-H in THF at 0 °C followed by quick separation over a neutral alumina column and subsequent recrystallization (Scheme 2). Under similar conditions, subporphyrin B-hydrides **8** and **10** were synthesized from **7** and **9** in 83% and 53% yields, respectively. The Lewis acidic nature of DIBAL-H is likely important in these reductions by facilitating liberation of the B-methoxy group from **1** (see Supporting Information, SI, for a possible reaction mechanism.

Scheme 1. Axial-Ligand Exchange Reactions of Subporphyrins

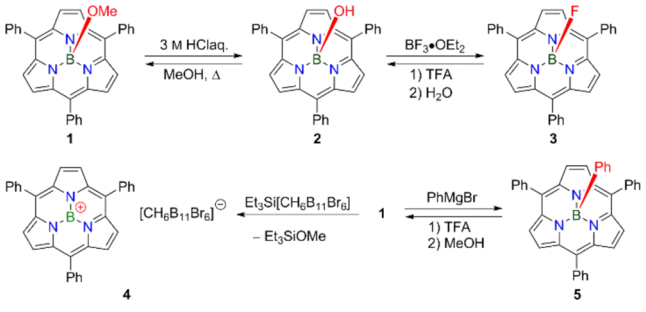

Scheme 2. Synthesis of Subporphyrin B-Hydrides

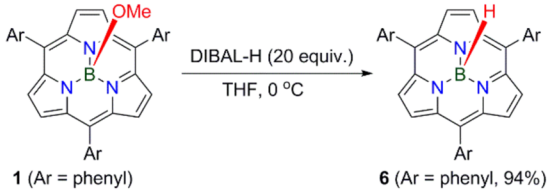

1 (Ar = phenyl)
7 (Ar = 4-methoxyphenyl)
9 (Ar = 4-bromophenyl)

6 (Ar = phenyl, 94%)
8 (Ar = 4-methoxyphenyl, 83%)
10 (Ar = 4-bromophenyl, 53%)

Received: December 12, 2014

DOI: 10.1021/ja5126269
J. Am. Chem. Soc. XXXX, XXX, XXX−XXX

Scheme S10). The importance of employing a Lewis acidic hydride source was confirmed by reduction of **1** with AlH_3 generated from $LiAlH_4$ and $AlCl_3$,[7] which gave **6** in 76% yield. This method was used for preparation of subporphyrin B-deuteride **6-*D*** in 74% yield.

High resolution atmospheric pressure chemical ionization-time-of-flight mass spectroscopy (HR-APCI-TOF-MS) operating in negative ion mode revealed the parent anion peak of **6** at m/z = 471.1920 (calculated for $[C_{33}H_{22}{}^{11}BN_3]^-$ = 471.1918) with an isotopic distribution consistent with the chemical composition. In the ^{1}H NMR spectrum of **6** in $CDCl_3$, the B-hydride signal was observed as a broad quartet at −2.27 ppm with $^1J_{BH}$ = 152 Hz (^{11}B−^{1}H coupling) at 60 °C.[8] Upon decreasing temperature the quartet signal gradually coalesced to a broad singlet signal due to rapid quadrupole-induced spin relaxation at lower temperature.[9] In the ^{11}B-decoupled ^{1}H NMR spectrum of **6**, the B-hydride signal was observed as a singlet and the ^{1}H NMR spectrum of **6-*D*** is identical to that of **6** except for the absence of the B-hydride signal. The ^{1}H NMR chemical shifts have been calculated by density functional theory (DFT) using the gauge-including atomic orbital (GIAO)[10] method at the B3LYP/6-31G(d) level,[11] which predicts the chemical shift of the B-hydride of **6** to reside at −2.40 ppm which is consistent with the experimental value. The ^{11}B NMR spectrum of **6** in $CDCl_3$ showed a broad doublet at −19.7 ppm with $^1J_{HB}$ = 147 Hz at rt.[8] When comparing the respective ^{11}B chemical shifts of compounds **1** (−15.1 ppm), **2** (−15.6 ppm), **3** (−14.8 ppm), and **5** (−16.4 ppm), compound **6** indicates that an axial hydride is the most electron-donating among these axial substituents. The infrared spectra of **6** and **6-*D*** display B−H and B−D stretching vibrations at 2280 and 2186 cm^{-1}, and 1716 and 1690 cm^{-1}, respectively, which are smaller than those of the corresponding reported matrix isolated BH_3NH_3 (2427 and 2417 cm^{-1}) and BD_3ND_3 (1837 and 1817 cm^{-1}).[12] These results suggest weaker B−H and B−D bonds on **6** and **6-*D*** than the corresponding ammoniaboranes.

Structural confirmations of **6**, **8**, and **10** have been revealed by X-ray diffraction analyses of their single crystals.[13] The crystal structure of **6** contains two independent but similar bowl-shaped molecules in the unit cell, and one of them is indicated in Figure 1a. The bowl-depths, defined by the distance between the boron atom and the mean plane of the six peripheral β-carbons, are 1.353 and 1.344 Å, and the B−N bond lengths of **6** are in the range of 1.495−1.505 Å. These structural features are quite similar to those of **1**, thus indicating that the central B atom of **6** is sp^3 hybridized similarly to **1**. The crystal structures of **8** and **10** also reveal similar bowl-shaped structures. Importantly, the B−H has been confirmed by refinement of X-ray diffraction data owing to its electron-rich hydride character, which has allowed us to determine the B−H bond lengths to be 1.257(19) and 1.21(2) Å for **6** and 1.266(15) Å for **8**, being slightly longer than those of a previously reported standard ammoniaborane complex (1.15(3) and 1.18(3) Å).[14] These results indicate weaker B−H bonds of **6** and **8** compared to the ammoniaborane complex, consistent with the infrared analyses. In the course of this study, we have succeeded in the structural determination of subporphyrin B-fluoride **3**,[13] which was reported by Kobayashi et al. in 2009,[4c] but its solid state structure has remained elusive. The crystal structure of **3** contains two independent subporphyrin molecules in the unit cell. The bowl-depths are 1.294 and 1.305 Å, and the B−F bond lengths are 1.412(4) and 1.409(4) Å, which are comparable to those of dipyrromethene-coordinated difluoroboron complexes (1.39−1.40 Å).[15]

The Soret-like and Q-like bands of **6** are observed at 387 and 512 nm, with the fluorescence profile peaking at 560 nm with an absolute fluorescence quantum yield of 0.13. Figure 2a shows the absorption and fluorescence spectra of **1**, **3**, **5**, B-ethyl substituted subporphyrin **11**,[4e] and B-phenylethynyl substituted subporphyrin **12**.[4e] Both the Soret-like and Q-like bands are red-shifted in the order **3** < **1** < **12** < **5** < **6** < **11**, reflecting the increasing electron-donating abilities of the axial B-substituents. The fluorescence peaks are red-shifted similarly in the order **3** ≤ **1** < **12** < **5** < **6** < **11**. In line with these results, a plot of S_0−S_1 excitation energies versus Hammett inductive constants σ_I[17] of the axial B-substituents constitutes a good straight line fit (SI, Figure S4-2). Interestingly, the absorption spectrum of **8** exhibits an enhanced and red-shifted Soret-like and Q-like bands as compared with **6**, probably due to possible intramolecular charge transfer interaction. The fluorescence spectrum of **8** was observed at 583 nm with a quantum yield of 0.38. While

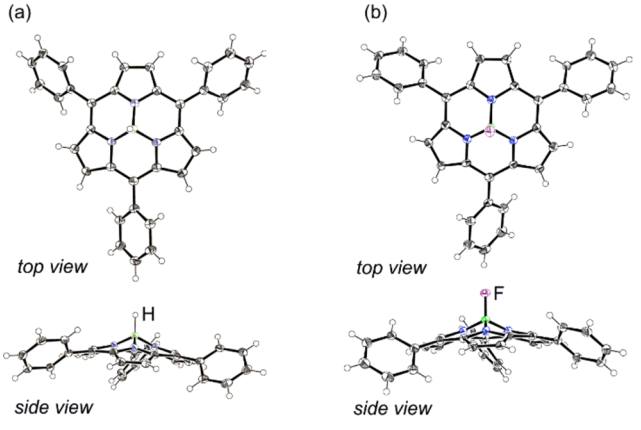

Figure 1. X-ray crystal structures of **6** (a) and **3** (b). Thermal ellipsoids are scaled to 50% probability. Solvent molecules are omitted for clarity.

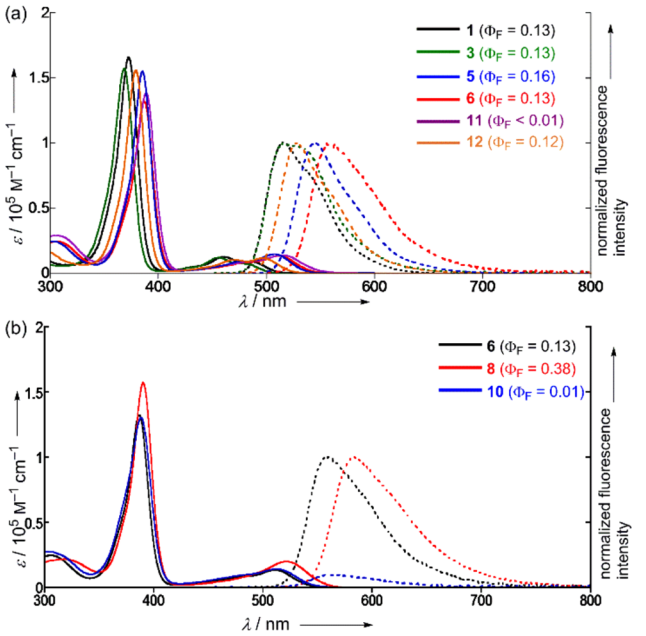

Figure 2. UV−vis absorption (solid lines) and fluorescence (dashed lines) spectra in CH_2Cl_2. Fluorescence spectra were recorded upon excitation at the peak maxima of each Soret-like bands.

DOI: 10.1021/ja5126269
J. Am. Chem. Soc. XXXX, XXX, XXX−XXX

subporphyrin **10** displayed an absorption spectrum that was very similar to that of **6**, its fluorescence spectrum was observed at 559 nm with a small fluorescence quantum yield (Φ_F = 0.01), apparently due to the effective intramolecular heavy atom effect of the bromine substituents. The fluorescence decay profiles of **6** and **6-*D*** measured by time-correlated single photon counting techniques were well-fitted with a single exponential function with time constants of 2.9 and 3.1 ns, respectively, which is quite similar to that of **1** (τ = 2.95 ns)[2b] and slightly larger than that of **5** (τ = 2.44 ns).[4e]

The oxidation and reduction potentials of **6** were measured by cyclic voltammetry along with those of **1**, **3**, and **5**. The first oxidation of **6** was observed as an irreversible wave at 0.36 V, being lower than the values seen for **1** (0.75 V), **3** (0.84 V), and **5** (0.58 V), again reflecting the electron-donating power of the B-hydride. In contrast, the first reduction potentials did not show significant differences: −1.95 V for **1**; −1.93 V for **3**; −2.01 V for **5**; −1.96 V for **6**. The DFT calculations indicated that only the a_1 symmetric HOMO has large electron coefficients at the boron center, and HOMO−1 and LUMOs have a node at the boron center (SI, Figure S9).[17] These frontier orbital features suggest that changes of the axial B-substituents alter the energy level of HOMO while the energy levels of the other frontier orbitals are left unchanged. Namely, the attachment of an electron-donating B-substituent lifts the energy level of the HOMO and decreases the HOMO−LUMO gap. These theoretical predictions are nicely consistent with the experimental photophysical and electrochemical spectroscopic observations.

Finally, the chemical reactivity of **6** was studied. Subporphyrin **6** was gradually hydrolyzed to **2** via reaction with adventitious water with concomitant formation of molecular hydrogen gas, as observed by ^{1}H NMR spectroscopy (SI, Figure S3-5). The hydrolysis rapidly proceeded by washing with an aqueous HCl solution (Scheme 3). However, in the solid state under a nitrogen atmosphere, **6** is stable and storable over several weeks without change.

Scheme 3. Hydrolysis of 6

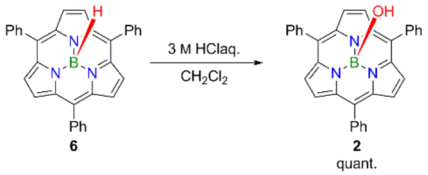

In the next step, hydroborations of aldehyde and imine with **6** were examined. The reaction of 3,5-di-*tert*-butylbenzaldehyde (**13**) with **6** (1.1 equiv) in C_6D_6 at rt was very slow, giving only a trace amount of the desired product **14** forming after 24 h (Scheme 4). Interestingly, the reaction was dramatically accelerated and completed in 5 min in the presence of 5 mol % of $Ph_3C[B(C_6F_5)_4]$ to give **14** in 94% yield along with Ph_3CH in 5% yield (^{1}H NMR yields) (Scheme 4). Product **14** was actually isolated in 75% yield through separation over a short silica gel column, and its structure was confirmed by X-ray diffraction analysis (Figure 3). Similarly, the reaction of benzophenone imine (**15**) with **6** in C_6D_6 gave subporphyrin B-(diphenylmethyl)amide **16**. The ^{1}H NMR spectrum of the reaction mixture revealed two doublets at −2.36 and 2.44 ppm (by $^3J_{HH}$ = 6.12 Hz) due to the amine and methylene protons of **16** (SI, Figure S3-20). The large high-field shifts of these protons are likely due to the close proximity of the diatropic ring current

Scheme 4. Hydroboration of Arylaldehyde and Imine with 6[a]

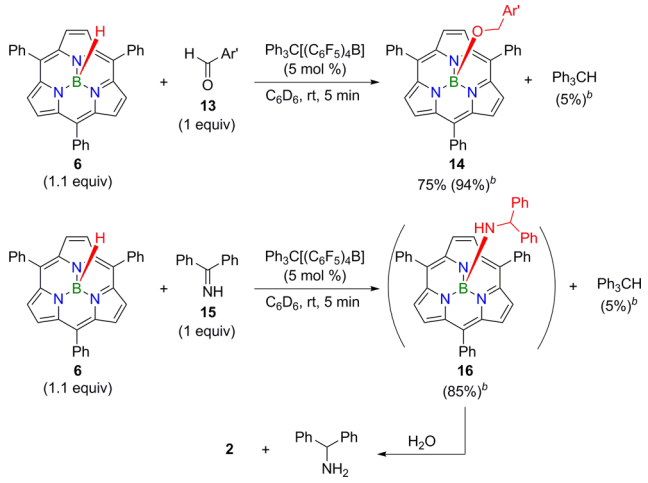

[a]Ar′ = 3,5-di-*tert*-butylphenyl. [b] Yields in parentheses were determined by ^{1}H NMR spectroscopy using $C_2H_2Cl_4$ as an internal standard.

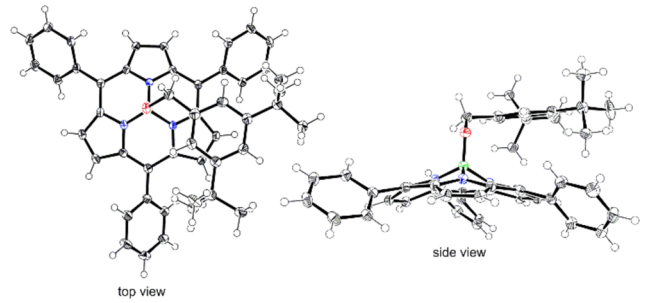

Figure 3. X-ray crystal structure of **14**. Thermal ellipsoids are scaled to 50% probability. Solvent molecules are omitted for clarity.

of the subporphyrin core. In addition, the ^{11}B NMR spectrum of **16** displayed a broad signal at −16.1 ppm coupled with the amine protons. Importantly, product **16** is the first example of subporphyrins bearing an axial B−N bond. Unfortunately, however, all attempts to isolate **16** were unsuccessful so far due to its extremely high hydrolytic reactivity.

A plausible reaction mechanism for the reduction of benzaldehyde with **6** is shown in Scheme 5. The reaction is initiated by abstraction of the hydride of **6** by the trityl cation to generate subporphyrin borenium cation **A**, which activates

Scheme 5. A Plausible Reaction Mechanism for Lewis Acid Catalyzed Hydroboration of Arylaldehyde with 6

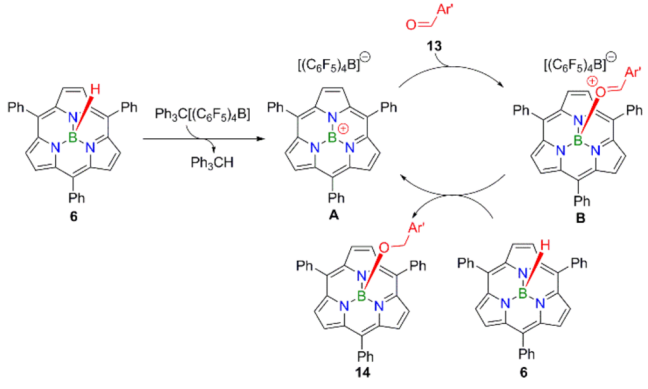

DOI: 10.1021/ja5126269
J. Am. Chem. Soc. XXXX, XXX, XXX−XXX

aldehyde **13** to form cationic intermediate **B**. Subsequent hydride transfer from **6** to **B** gives product **14** with reproduction of **A**. The initiation step was actually confirmed by reaction of **6** with a stoichiometric amount of $Ph_3C[B(C_6F_5)_4]$ in CD_2Cl_2, which led to the quantitative formation of subporphyrin borenium cation tetrakis(pentafluorophenyl)borate salt and Ph_3CH (SI, Figure S3-22). A similar reaction involving a borenium cation as a reaction intermediate for imine hydroboration has been recently revealed by Crudden et al.[18]

In summary, the subporphyrin B-hydrides **6**, **8**, and **10** were prepared for the first time by the reduction of subporphyrin B-methoxides **1**, **7**, and **9** with DIBAL-H and were fully characterized. Red shifts in the Soret-like and Q-like bands and fluorescence emission of the subporphyrin B-hydrides are accounted for in terms of the electron-donating nature of the B-hydride that lifts the energy level of the HOMO while leaving other frontier orbitals almost unaffected. The hydridic nature of **6** has been demonstrated by the production of H_2 from the reaction with water or HCl as well as the reductions of aromatic aldehydes and imines in the presence of a catalytic amount of $Ph_3C[B(C_6F_5)_4]$. Study on the exploration of novel reactivities of **6** is worthy of further investigation.

■ ASSOCIATED CONTENT

Supporting Information

Detailed experimental conditions and procedures, analytical data, theoretical details, and crystallographic data for compounds **8** and **10**. This material is available free of charge via the Internet at http://pubs.acs.org.

■ AUTHOR INFORMATION

Corresponding Authors

*osuka@kuchem.kyoto-u.ac.jp
*dongho@yonsei.ac.kr

Notes

The authors declare no competing financial interest.

■ ACKNOWLEDGMENTS

The work at Kyoto was supported by JSPS KAKENHI Grant Numbers 25220802 and 25620031. The work at Yonsei was supported by Global Research Laboratory (GRL) Program (2013-8-1472) of the Ministry of Education, Science, and Technology (MEST) of Korea.

■ REFERENCES

(1) (a) Inokuma, Y.; Osuka, A. *Dalton Trans.* **2008**, 2517. (b) Osuka, A.; Tsurumaki, E.; Tanaka, T. *Bull. Chem. Soc. Jpn.* **2011**, *84*, 679. (c) Claessens, C. G.; González-Rodríguez, D.; Rodríguez-Morgade, M. S.; Medina, A.; Torres, T. *Chem. Rev.* **2014**, *114*, 2192.

(2) (a) Inokuma, Y.; Kwon, J. H.; Ahn, T. K.; Yoo, M.-C.; Kim, D.; Osuka, A. *Angew. Chem., Int. Ed.* **2006**, *45*, 961. (b) Inokuma, Y.; Yoon, Z. S.; Kim, D.; Osuka, A. *J. Am. Chem. Soc.* **2007**, *129*, 4747. (c) Tsurumaki, E.; Saito, S.; Kim, K. S.; Lim, J. M.; Inokuma, Y.; Kim, D.; Osuka, A. *J. Am. Chem. Soc.* **2008**, *130*, 438. (d) Tsurumaki, E.; Inokuma, Y.; Easwaramoorthi, S.; Lim, J. M.; Kim, D.; Osuka, A. *Chem.—Eur. J.* **2009**, *15*, 237. (e) Hayashi, S.; Tsurumaki, E.; Inokuma, Y.; Kim, P.; Sung, Y. M.; Kim, D.; Osuka, A. *J. Am. Chem. Soc.* **2011**, *133*, 4254. (f) Majima, Y.; Ogawa, D.; Iwamoto, M.; Azuma, Y.; Tsurumaki, E.; Osuka, A. *J. Am. Chem. Soc.* **2013**, *135*, 14159.

(3) (a) Kobayashi, N.; Takeuchi, Y.; Matsuda, A. *Angew. Chem., Int. Ed.* **2007**, *46*, 758. (b) Takeuchi, Y.; Matsuda, A.; Kobayashi, N. *J. Am. Chem. Soc.* **2007**, *129*, 8271. (c) Xu, T.; Lu, R.; Liu, X.; Chen, P.; Qiu, X.; Zhao, Y. *Eur. J. Org. Chem.* **2008**, 1065.

(4) Selected papers focused on boron-axial ligand exchange reactions of subporphyrins: (a) Inokuma, Y.; Osuka, A. *Chem. Commun.* **2007**, 2938. (b) Inokuma, Y.; Osuka, A. *Org. Lett.* **2008**, *10*, 5561. (c) Shimizu, S.; Matsuda, A.; Kobayashi, N. *Inorg. Chem.* **2009**, *48*, 7885. (d) Tsurumaki, E.; Hayashi, S.; Tham, F. S.; Reed, C. A.; Osuka, A. *J. Am. Chem. Soc.* **2011**, *133*, 11956. (e) Saga, S.; Hayashi, S.; Yoshida, K.; Tsurumaki, E.; Kim, P.; Sung, Y. M.; Sung, J.; Tanaka, T.; Kim, D.; Osuka, A. *Chem.—Eur. J.* **2013**, *19*, 11158.

(5) (a) Meller, A.; Ossko, A. *Monatsh. Chem.* **1972**, *103*, 150. (b) Claessens, C. G.; González-Rodríguez, D.; Torres, T. *Chem. Rev.* **2002**, *102*, 835.

(6) (a) Brothers, P. J. *Chem. Commun.* **2008**, 2090. (b) Brothers, P. J. *Inorg. Chem.* **2011**, *50*, 12374. (c) Albrett, A. M.; Boyd, P. D. W.; Clark, G. R.; Gonzalez, E.; Ghosh, A.; Brothers, P. J. *Dalton Trans.* **2010**, *39*, 4032. Related dipyrromethene-based B-hydrides were reported: (d) Piers; Bonnier, C.; Piers, W. E.; Parvez, M.; Sorensen, T. S.; et al. *Chem. Commun.* **2008**, 4593.

(7) AlH_3 was generated *in situ* by the reaction of $LiAlH_4$ and $AlCl_3$ (0.33 equiv vs. $LiAlH_4$) and then treated with **6** at 0 °C: Finholt, A. E.; Bond, A. C., Jr.; Schlesinger, H. I. *J. Am. Chem. Soc.* **1947**, *69*, 1199.

(8) NMR simulations were performed using WinDNMR software for estimations of the coupling constants of $^1H—^{11}B$. See Figures S3−S4 in: Reich, H. J. *J. Chem. Educ.* **1995**, *72*, 1089.

(9) (a) Beall, H.; Bushweller, C. H.; Dewkett, W. J.; Grace, M. *J. Am. Chem. Soc.* **1970**, *92*, 3484. (b) Marynick, D.; Onak, T. *J. Chem. Soc. A* **1970**, 1160. (c) Bushweller, C. H.; Beall, H.; Grace, M.; Dewkett, W. J.; Bilofsky, H. S. *J. Am. Chem. Soc.* **1971**, *93*, 2145.

(10) Magyarfalvi, G.; Wolinski, K.; Hinton, J.; Pulay, P. *eMagRes.* **2011**, DOI: 10.1002/9780470034590.emrstm0501.pub2.

(11) Optimizations and single-point calculations were performed using the Gaussian 09 package: Gaussian 09, Revision A.02. The full list of the authors is given in the SI.

(12) Smith, J.; Seshadri, K. S.; White, D. *J. Mol. Spectrosc.* **1973**, *45*, 327.

(13) Crystallographic data for **6**: $2(C_{33}H_{22}BN_3)CH_2Cl_2$, M_w = 1027.62, monoclinic, $P2_1/c$, a = 9.698(2) Å, b = 25.028(7) Å, c = 21.752(5) Å, β = 98.422(5)°, V = 5223(2) Å^3, D_c = 1.307 g/cm^3, Z = 4, R_1 = 0.0536 ($I > 2.0\,\sigma(I)$), wR_2 = 0.1354 (all data), GOF = 1.044 ($I > 2.0\,\sigma(I)$), CCDC; 1036910. **3**: $2(C_{33}H_{21}BFN_3)CH_2Cl_2$, M_w = 1063.60, monoclinic, $P2_1/c$, a = 9.667(3) Å, b = 25.121(8) Å, c = 21.748(7) Å, β = 98.248(10)°, V = 5227(3) Å^3, D_c = 1.352 g/cm^3, Z = 4, R_1 = 0.0646 ($I > 2.0\,\sigma(I)$), wR_2 = 0.1609 (all data), GOF = 1.039 ($I > 2.0\,\sigma(I)$), CCDC; 1036913. **14**: $C_{48}H_{44}BN_3O$, M_w = 689.67, triclinic, $P\bar{1}$, a = 10.0454(19) Å, b = 12.488(3) Å, c = 15.612(2) Å, α = 71.341(14)°, β = 74.45(3)°, γ = 83.50(3)°, V = 1786.8(6) Å^3, D_c = 1.282 g/cm^3, Z = 2, R_1 = 0.0486 ($I > 2.0\,\sigma(I)$), wR_2 = 0.1314 (all data), GOF = 1.007 ($I > 2.0\,\sigma(I)$), CCDC; 1036914. Crystallographic data for **8** (CCDC; 1036911) and **10** (CCDC; 1036912) are given in the Supporting Information.

(14) Klooster, W. T.; Koetzle, T. F.; Siegbahn, P. E. M.; Richardson, T. B.; Crabtree, R. H. *J. Am. Chem. Soc.* **1999**, *121*, 6337.

(15) Bröring, M.; Krüger, R.; Link, S.; Kleeberg, C.; Köhler, S.; Xie, X.; Ventura, B.; Flamigni, L. *Chem.—Eur. J.* **2008**, *14*, 2976.

(16) Hansch, C.; Leo, A.; Taft, R. W. *Chem. Rev.* **1991**, *91*, 165.

(17) Gouterman, M. *J. Mol. Spectrosc.* **1961**, *6*, 138.

(18) Eisenberger, P.; Bailey, A. M.; Crudden, C. M. *J. Am. Chem. Soc.* **2012**, *134*, 17384.

DOI: 10.1021/ja5126269
J. Am. Chem. Soc. XXXX, XXX, XXX−XXX